Molecular Crystals and Liquid Crystals
Publication details, including instructions for authors and subscription information:
http://www.tandfonline.com/loi/gmcl20

Polarization and Spectral Properties of a Cholesteric Liquid Crystal Fabry-Perot Slab

Karen Allahverdyan [a b], Ashot Gevorgyan [b], Tigran Galstian [a] & Rafik Hakopyan [b]

[a] Center for Optics, Photonics and Laser, Department of Physics, Engineering Physics and Optics, Laval University, Pav. d'Optique-Photonique, 2375 Rue de la Terrasse, Québec, G1V 0A6, Canada

[b] Department of Physics, Yerevan State University, 1 Alex Manoogian, 0025, Yerevan, Armenia

Version of record first published: 15 May 2012.

To cite this article: Karen Allahverdyan , Ashot Gevorgyan , Tigran Galstian & Rafik Hakopyan (2012): Polarization and Spectral Properties of a Cholesteric Liquid Crystal Fabry-Perot Slab, Molecular Crystals and Liquid Crystals, 560:1, 23-34

To link to this article: http://dx.doi.org/10.1080/15421406.2012.661955

Mol. Cryst. Liq. Cryst., Vol. 560: pp. 23–34, 2012

ISSN: 1542-1406 print/1563-5287 online
DOI: 10.1080/15421406.2012.661955

Taylor & Francis
Taylor & Francis Group

Polarization and Spectral Properties of a Cholesteric Liquid Crystal Fabry-Perot Slab

KAREN ALLAHVERDYAN,[1,2] ASHOT GEVORGYAN,[2]
TIGRAN GALSTIAN,[1,*] AND RAFIK HAKOPYAN[2]

[1]Center for Optics, Photonics and Laser, Department of Physics, Engineering Physics and Optics, Laval University, Pav. d'Optique-Photonique, 2375 Rue de la Terrasse, Québec, G1V 0A6, Canada
[2]Department of Physics, Yerevan State University, 1 Alex Manoogian, 0025 Yerevan, Armenia

We report the creation of a double-feedback optical element based on a Fabry-Perot cavity filled with a planar aligned cholesteric liquid crystal mixture. The reflection band of the liquid crystal is in the near infra-red region. The polarization and spectral properties of this element are characterized experimentally and simulated theoretically. Preliminary experimental results are obtained for the transmission's dependence upon the orientation of the linear polarisation plane and the polarization state of the incident probe beam, with a wavelength out of resonance. The corresponding theoretical simulation results are in qualitative agreement with the experimental results.

Keywords Cholesteric liquid crystals; distributed feedback; dual frequency liquid crystal; electrooptic switch; Fabry-Perot resonator; liquid crystals; polarimetry; resonant reflection

Introduction

Cholesteric liquid crystals (CLC) are fascinating examples of molecular self-organization into helicoidal (chiral) quasi-macroscopic structures generating wavelength and polarization selective reflection [1–4]. They have generated important promise of applications in light reflectors and polarization-free modulators. Indeed, significant effort was devoted to manipulate their reflective properties, such as reflection strength, bandwidth, etc. (see, e.g., [5–14] and references therein).

The electrical modulation tool being very interesting (from practical point of view), we have focused our efforts on achieving a fast electrical modulation of the reflection of the CLC by destroying and then restoring its helix as quickly as possible [15]. To achieve that goal, we have used a mixture of a CLC and a dual frequency nematic liquid crystal (DF-NLC), see later. The addition of the DF-NLC has shifted the resonant reflection band into near infra-red spectral band. The commercially purchased Indium Tin Oxide (ITO) layers being optimized only for the visible spectral band, the spectral analyses of obtained cells

*Address correspondence to Tigran Galstian, Center for Optics, Photonics and Laser, Department of Physics, Engineering Physics and Optics, Laval University, Pav. d'Optique-Photonique, 2375 Rue de la Terrasse, Québec, G1V 0A6, Canada. Phone: 1-418-6562025. E-mail: galstian@phy.ulaval.ca

has shown very strong Fabry-Perot oscillations overlapping with the resonant reflection band of the CLC. We have obtained thus a double-feedback system, the first one thanks to the classical Fabry-Perot effect and the second one due to the distributed feedback of the helicoidal structure of the CLC. The present work describes the preliminary results of the linear characterization of the obtained cells from spectral and polarization points of view.

Materials and Cells

The material compositions used as well as the cell fabrication are described in details in the Ref. [15]. In a very short description: the material was obtained by mixing two materials: the CLC, called CB15, and the DF-NLC, called MLC 2048, (both purchased from Merck). The final compound (studied in the present work) contains 33 wt % of CB15 and 67 wt% of MLC 2048. The choice of those compounds was based on the desired dielectric parameters as well as the material availability. The MLC 2048 is a well-known material (see, e.g., [16]). To the best of our knowledge, the compound CB15 is less known (see, e.g., [14,17,18]). Planar aligned cells of 5 μm thickness were fabricated by using two antiparallel rubbed Polyimide (PI-150, from Nissan) coated substrates.

Spectral Characterization

The transmission spectra of above mentioned cells were measured by using a spectrophotometer (model Varian Cary 500 scan). There was no polarizer or wave plate used in this measurement. The probe light was thus almost non polarized (except the residual anisotropic influence of optical elements placed on the path of the probe beam of the spectrophotometer). The obtained results show that the resonant reflection band of the CLC mixture is in the range from 1450 nm to 1650 nm (Fig. 1). However, the transmission spectra of cells show also strong Fabry-Perot type oscillations in the spectral neighbourhood of the resonant reflection band of the CLC mixture (Fig. 1). The application of a strong electrical field (SIN shaped AC voltage of 50V RMS, at 1 kHz) destroys the CLC helix and we observe only the Fabry-Perot oscillations (Fig. 1). Those oscillations are spectrally shifted because

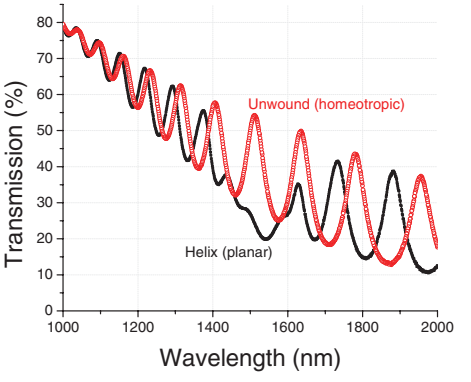

Figure 1. Cholesteric liquid crystal cell's transmittance spectrum (measured with a non-polarized light, see text for details) with and without the unwinding electric field applied. Cell thickness is 5 μm, molecular orientation on the substrate surfaces is planar.

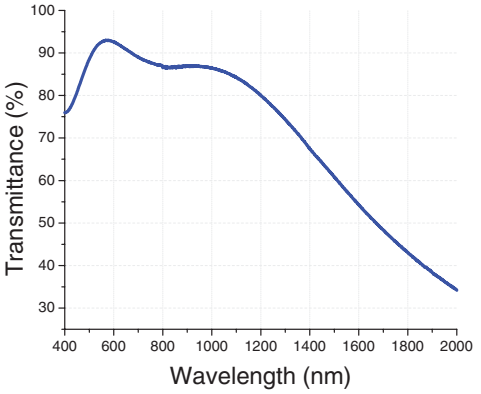

Figure 2. The transmittance spectrum of the ITO coated glass substrate, measured in air.

of the change of the effective refractive index of the unwound (homeotropic) molecular orientation.

The observed Fabry-Perot effect was the reason why the transmission of the ITO coated glasses (used to build our cells) was characterized separately in the broad spectral range. The obtained results (see Fig. 2) show that the light transmission is significantly reduced in the near infra-red range of wavelengths. This is very likely because of both the ITO absorption as well as the index mismatch between various adjacent optical layers (We have measured the transmission and reflection coefficients (for $\lambda = 1481$ nm wavelength) of ITO coated glass we used. Here are the obtained results: the reflexion $\boldsymbol{R} = 0.2$ and the transmission $\boldsymbol{T} = 0.61$. So they are both higher in fnra-red region then in visible region.)

As we have already mentioned, the obtained cell is thus a rather complex element since it is characterized by two feedback mechanisms. The optical properties in such structure may be very complex, particularly the dependence of its transmission from light's wavelength and polarization. This is because both phenomena are wavelength dependent. In addition, if the Fabry-Perot effect may be considered as polarization independent (for normal incidence and for a non gyrotropic material inside); in contrast, the CLC has strongly polarization dependent (gyrotropic) properties.

We have thus proceeded to the experimental characterization of this structure. We have also performed a very preliminary theoretical modeling of the cell. This modeling succeeds to reproduce qualitatively the observed transmission of our structure in unpolarized white light, Fig. 3. The corresponding details (of the theoretical analyses) will be presented later. For the moment, the values of parameters, used for this modeling, are as follows: ordinary refractive index $\boldsymbol{n_o} = 1.5$, extraordinary refractive index $\boldsymbol{n_e} = 1.7$, helix pitch $\boldsymbol{p} = 0.96\ \mu$m (the distance in which the LC molecules realise an entire rotation at 360°) and the number of entire helixes $\boldsymbol{t} = 6$. Since the Fabry–Perot effect is significant in this specific case, it is important to choose correct parameters conditioning all reflections (e.g., the effective refractive indexes $\boldsymbol{n}$ and the effective thicknesses $\boldsymbol{d}$). Based on the observed transmission spectrum of the ITO coated glass (Fig. 2), where the curve is nearly linear in the range from 1000 nm to 2000 nm, we supposed that the effective refractive index $\boldsymbol{n}$ is also changing linearly. By varying these two parameters ($\boldsymbol{n}$ and $\boldsymbol{d}$) we have chosen ones, which fit better with our experimental curve (Fig. 3): $\boldsymbol{n} = 1.4 + 2(\lambda - 1)/\lambda$, $\boldsymbol{d} = 1$ um. We have obtained a rather qualitative agreement and we have used the above mentioned parameters in our further theoretical simulations.

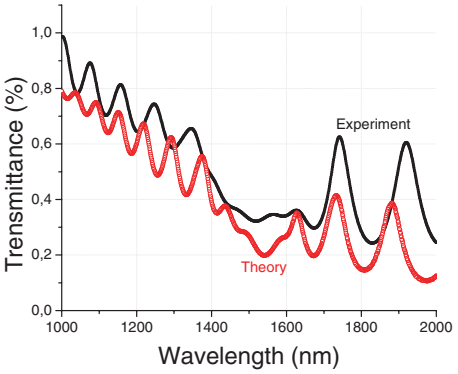

Figure 3. The CLC cell's transmittance spectrum (theory and experiment) for unpolarized broadband (white light) probe beam.

Experimental Set-Up

The polarization dependence of the transmission of our structure was studied in two different set-ups. First, we have built a simple set-up (Fig. 4) to study the transmission dependence of the linearly polarized narrow band light upon the orientation of its polarization plane with respect to the input orientation of the CLC's director (average orientation of long molecular axes, [1]), defined by the rubbing direction of the Polyimide layers.

In this experiment, a diode HP 8155A laser diode source, operating between 1300 nm and 1321 nm wavelength, was used. That source was coupled to a single mode SMF28 fiber. This wavelength was not exactly inside the resonant reflection band, but was near its short wavelength wing. The fiber's output beam was collimated with the lens (Fig. 4), passed through the Polarizer 1, then through a planar aligned nematic liquid crystal (NLC) cell, which was used as an electrically variable retardation plate. Namely, the NLC cell's rubbing direction was oriented to 45° with respect to the first polarizer's transmission axis. Thus, for an appropriate applied voltage (from an electrical generator U), the NLC cell's optical path difference (defined by the effective birefringence and the thickness of the cell) corresponds to a quarter wave plate, and it changes thus the probe light's polarisation into circular polarization. Keeping that voltage stable, during the experiment, the Polarizer 2 was gradually rotated, changing thus the incident light's polarization plane, while keeping

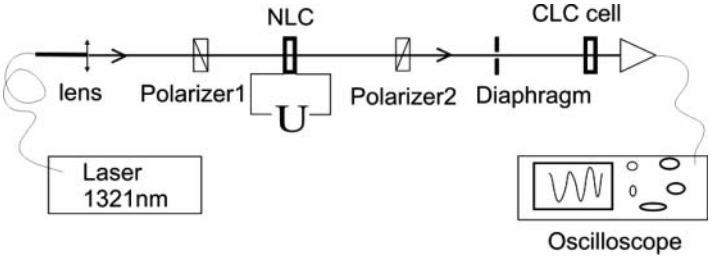

Figure 4. Schematic representation of the experimental setup for the study of the cholesteric liquid crystal cell transmission's dependence upon the plane polarized probe light's electric field orientation with respect to the director's orientation on the substrates.

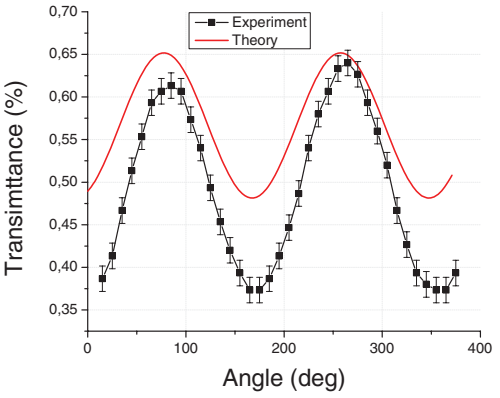

Figure 5. The CLC cell's transmission dependence upon the angle between the linearly polarized light's polarization direction and the substrates' rubbing direction (defining the director's orientation on the surfaces).

its power constant. Then the transmitted, through the CLC cell, light's power was measured by the photodectecor PD.

Experimental and Simulation Results

Figure 5 shows the transmittance dependence upon the angle between the probe light's polarization plane and the rubbing direction of the cell (theory end experiment). We see, in the Fig. 5, that the transmission variations upon the incident light polarization plane has a periodical nature with a period of 180°, which is quite normal as the incident beam polarization stays the same if we turn the Polarizer 2 to 180°. We see also, that the transmission is minimal for the 0° angle, which corresponds to the incident beam of extra ordinary type (polarized in the same plane as the rubbing direction defining the input orientation of the CLC's director). In contrast, the transmission is maximum for the input probe light of ordinary polarization (polarized perpendicular to the rubbing direction).

The transmission dependence of the cell was also measured versus the polarization state of the incident beam. Namely, here we changed not only the angle of the polarisation plane of the probe light, but also its elipticity (from circular left—elliptical—linear—elliptical—circular right, etc.). The previous experimental set-up was slightly changed to perform this experiment (Fig. 6). We have added a glass beam splitter, the second Polarizer 2 and a second photodetector (PD2), which were used to monitor, in real time, the incident (on the CLC cell) light's polarisation state. The Polariser 2 was always crossed with the Polarizer 1 and the NLC cell's director was oriented at 45° with respect to the first polarizer's transmission axis (the transmission axis of the Polarizer 1 was set vertical). Thus, the PD2's detected "reference" signal having a minimum value corresponds to the linearly polarized probe light (incident on the CLC cell) oriented in the vertical plane and the detected maximum signal corresponds to the linearly polarized light oriented in the horizontal plane (Fig. 3). The CLC cell's rubbing direction was set horizontal.

During the experiment we increased gradually the voltage U (applied to the NLC cell), which changed the NLC cell's effective birefringence, and, as a result, the probe light's polarisation state was gradually changed at the input of the CLC cell. We registered the transmitted (through the CLC cell) light's power (by **PD1)** upon the applied, to the NLC

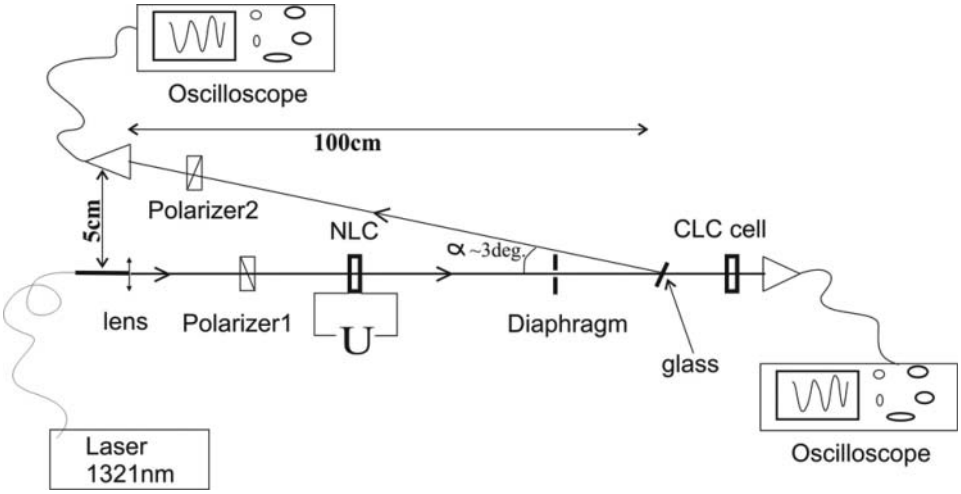

Figure 6. Schematic representation of the experimental setup for the study of the cell's transmission dependence upon the probe light's polarization state.

cell, voltage. During those changes, the signal, detected by the PD2 was also monitored to follow the dynamic change of the polarization state of the probe beam. This signal was used as reference (Fig. 7).

The obtained results (for both signals) are shown in the Fig. 7. As one can see, there are multiple cycles of changes of the polarization state of the probe beam for the applied voltage range (below 7.5 V). The transmission dependence shows oscillations correlated with those cycles. There is almost 50% variation of the probe beam transmission depending upon the orientation of the plane of the input polarization. There is also some noticeable shift between the two oscillations (signal and reference).

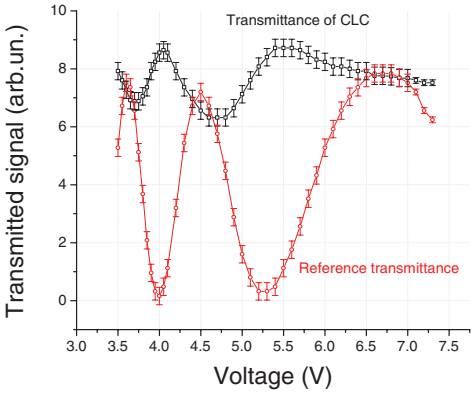

Figure 7. CLC cell's transmission dependence upon the voltage, applied on the variable retardation NLC cell. The "reference transmittance" curve allows the monitoring of the corresponding polarization state of the probe beam. The Minimums and Maximums of this curve correspond to the linearly polarized probe beam with its polarization plane being, respectively; perpendicular and parallel to the cell's rubbing direction (see the text for details). The first polarizer is aligned at 90°.

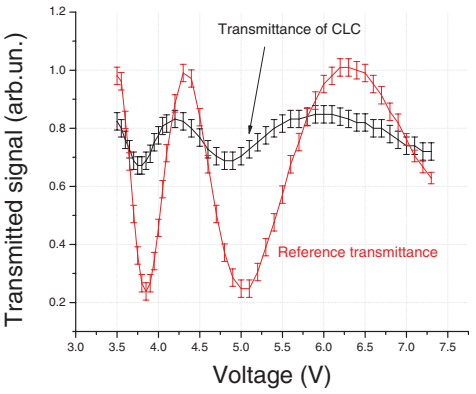

Figure 8. CLC cell's transmission dependence upon the voltage, applied on the variable retardation NLC cell (see the text for more details). The first polarizer is aligned at 30°.

Some additional experiments have been performed too. Thus we have first turned the Polarizer 1, the NLC cell' rubbing direction and the Polarizer 2 to 60° (Fig. 8) and then to another 30° (Fig. 9), and then we repeated the above mentioned measurements. As we can see, in Figs 8 and 9, depending upon the incident azimuthal angle (the angle between the probe beam's polarization and the input orientation of the CLC's director, when the beam is linearly polarized), the transmission changes significantly: the transmitted (through the CLC cell) power's maximum and minimum conditions are changed, and also the amplitude of the transmitted light's oscillations is changed significantly. Let us remind that, in the Fig. 8, the minimum of the reference curve corresponds to the linearly polarized probe light with an azimuthal angle of 30° (with respect to the input orientation of the director), and the Fig. 9 corresponds to the azimuthal angle of 0° (with respect to the input orientation of the director).

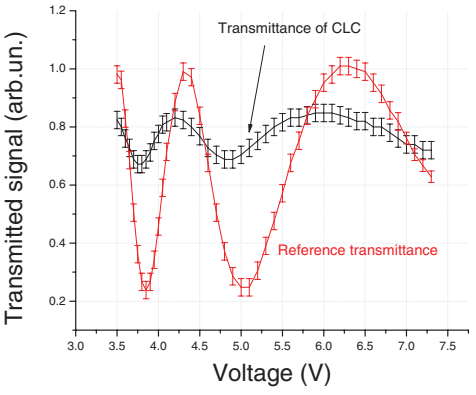

Figure 9. CLC cell's transmission dependence upon the voltage, applied on the variable retardation NLC cell. The "reference transmittance" curve allows the monitoring of the corresponding polarization state of the probe beam. The Minimums and Maximums of this curve correspond to the linearly polarized probe beam with its polarization plane being, respectively; parallel and perpendicular to the cell's rubbing direction (see the text for details). The first polarizer is aligned at 0°.

The Theoretical Method of Analysis

Corresponding theoretical simulations have been done trying to reproduce the experimentally observed dependences of the probe light transmission upon its state of polarization. The problem was solved by Ambartsumian's layer addition modified method [19, 20] adjusted to the solution of such problems. Namely, let us represent the solution of the boundary problem of light transmission through the multi-layer system in the following form:

$$\vec{E}_r = \hat{R}\vec{E}_i, \quad \vec{E}_t = \hat{T}\vec{E}_i, \tag{1}$$

where the indices i, r and t denote the incident, reflected and transmitted waves' fields, $\hat{R}$ and $\hat{T}$ are the reflection and transmission matrices, and $E^p_{i,r,t}$ and $E^s_{i,r,t}$ are corresponding amplitudes of the incident, reflected and transmitted waves: $\vec{E}_{i,r,t} = E^p_{i,r,t}\vec{n}_p + E^s_{i,r,t}\vec{n}_s = [\begin{smallmatrix} E^p_{i,r,t} \\ E^s_{i,r,t} \end{smallmatrix}]$, where $\vec{n}_p$ and $\vec{n}_s$ are the unit vectors of orthogonal linear polarizations.

According to Ambartsumian's layer addition modified method, if there is a system consisting of two adjacent (from left to right) layers, A and B, then the reflection transmission matrices of the system, $A + B$, viz. $\widehat{R}_{A+B}$ and $\widehat{T}_{A+B}$, are determined in terms of similar matrices of its component layers by the matrix equations:

$$\begin{aligned} \widehat{R}_{A+B} &= \widehat{R}_A + \tilde{\widehat{T}}_A \widehat{R}_B [\widehat{I} - \tilde{\widehat{R}}_A \widehat{R}_B]^{-1} \widehat{T}_A, \\ \widehat{T}_{A+B} &= \widehat{T}_B [\widehat{I} - \tilde{\widehat{R}}_A \widehat{R}_B]^{-1} \widehat{T}_A, \end{aligned} \tag{2}$$

where the tilde denotes the corresponding reflection and transmission matrices for the reverse direction of light propagation, and $\hat{I}$ is the unit matrix. The exact reflection and transmission matrices for a finite CLC layer (at normal incidence) and an isotropic layer are well known [21, 22]. First, we attach the CLC layer with the isotropic layer (1) from the left side, using the matrix Eqs (2). In the second stage, we attach the isotropic layer (2) with the obtained CLC layer-isotropic layer (2) system. The ellipticity e and the azimuth ψ of the transmitted light are expressed by $\chi = E^s_t / E^p_t$ through the following formulae:

$$\psi = \frac{1}{2}\text{arctg}\left(\frac{2\text{Re}(\chi)}{1-|\chi|^2}\right), \qquad e = \frac{1}{2}\arcsin\left(\frac{2\text{Im}(\chi)}{1+|\chi|^2}\right). \tag{3}$$

We have already mentioned the parameter values, used for the theoretical fitting. Four different azimuthal angles of the incident light's polarization are thus shown in the Fig. 10. We can see that all the four curves are different from each other, and they coincide only when the ellipticity is equal to -1 or 1, i.e., when the probe's polarization is circular.

Another interesting point is the transmittance dependence upon the ellipticity of the input probe's polarization: neither of four curves is constant. Finally, transmission modulations are different for different azimuthal angles and the maximum or/and minimum transmission values are not obtained for the same ellipticity values, they also depend upon the azimuthal angle.

Figure 11 presents (in 3D and 2D forms) the result of the theoretical simulation for the dependence of the reflection spectra upon the refractive indexes of substrates of the cell. It shows, that the form of the spectra depends strongly upon the CLC cell's limiting substrates refractive index; thus the spectrum is "typical" (without Fabry-Perot oscillations, as we usually see in the literature) for refractive indexes near to the refractive indexes of

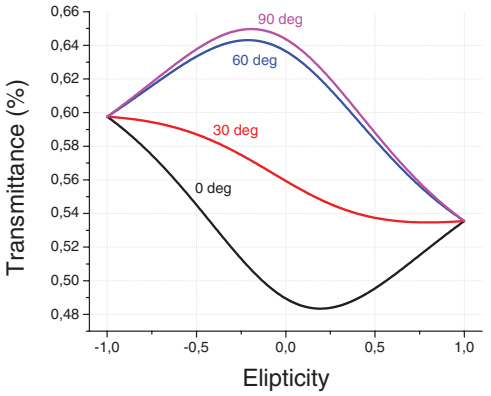

Figure 10. Theoretical simulation results for light transmittance's dependence upon the probe light polarization elipticity for four different fixed ellipse axes (the angles between the axis of the polarization ellipse and the rubbing direction are shown on each curve).

the CLC ($\sim 1 < n < \sim 2$). The Fabry—Perot effect appears for higher refractive indexes. This oscillation amplitude increases with the increase of substrates' refractive index.

Summary and Conclusions

The obtained experimental results confirm the complexity of polarization and spectral dependences of the double-feedback system composed of a Fabry-Perot cavity filled with planarly oriented CLC. The corresponding simulations are in qualitative agreement with those results. In fact, a closer look on the simulation results show that, in some cases, there is even a good quantitative agreement, for example, in the case of the transmission dependence upon the incidence azimuthal angle of the plane of the polarization of the probe beam (Fig. 7 vs Fig. 10). Namely, both the theory and experiments show a ratio of 1.3 for the transmittance of the plane polarized probe beam with its polarization aligned in vertical and horizontal directions. However, the same comparison for the two opposed circularly polarized probe beams gives the experimental ratio of 1.3 (see Figs 7 and 8) against the theoretical ratio of 1.13 (which is closer to the experimental value of 1.15 obtained in the Fig. 9).

The qualitative picture of spectral dependences is well represented by theoretical simulations. For example, the overlap of the Fabry-Perot effect with the resonant reflection of the CLC (Fig. 3) and the gradual appearance of the Fabry-Perot effect when introducing an index mismatch at substrates of the CLC cell (Fig. 11). However, the overall agreement between experimental and theoretical results is very qualitative and preliminary.

We have fabricated and characterized CLC cells exhibiting a double feedback phenomenon generated by the Fabry-Perot effect and the helicoidal structure of the CLC. We believe that this is a very interesting element and eventually it could be useful for various photonic applications (first of all for fast switching). A preliminary study (experimental and theoretical) was conducted, which provided only a qualitative agreement. Further study is required to better understand the key factors influencing the polarization and spectral properties of obtained elements.

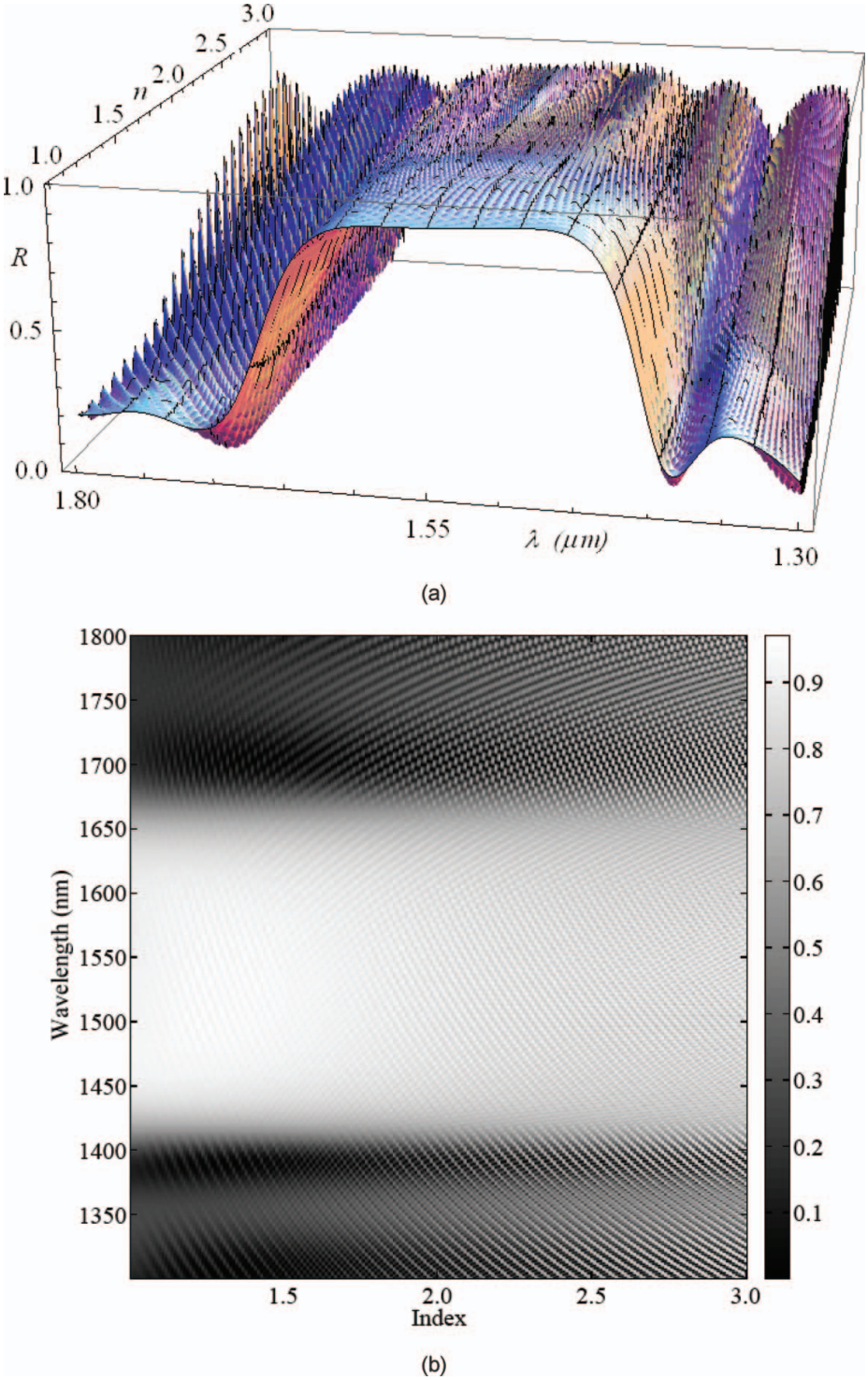

Figure 11. Theoretical simulation results describing (in *a)* 3D and *b)* 2D forms) the dependence of the CLC cell's reflection coefficient upon the probe wavelength and upon the substrates' refractive indexes for non-polarized probe light.

Acknowledgment

We would like to thank Professor Beliakov for discussions. We also thank the financial support of Canadian Institute for Photonic Innovations (CIPI), Fonds Québécois de la Recherche sur la Nature et les Technologies (FQRNT) and Natural Sciences and Engineering Research Council of Canada (NSERC).

References

[1] de Gennes, P. G., & Prost, J. (1995). *The Physics of Liquid Crystals*, Oxford University Press: 2nd Edition.

[2] Belyakov, V. A., Dmitrienko, V. E., & Orlov, V. P. (1979). Optics of cholesteric liquid crystals. *Soviet Physics Uspekhi*, *22*(2), (Sov. Phys. Usp. 22 64).

[3] Neville, A. C., & Caveney, S. (1969). Scarabaeid beetle exocuticle as an optical analogue of cholesteric liquid crystals. *Bid. Rev.*, *44*, 531–562.

[4] Sharma, V., Crne, M., Park, J. Ok., & Srinivasarao, M. (24 July 2009). Structural origin of circularly polarized iridescence in jeweled beetles. *Science*, *325*(5939), 449–451.

[5] Broer, D. J., Lub, J., & Mol, G. N. (30 November 1995). Wide-band reflective polarizers from cholesteric polymer networks with a pitch gradient. *Nature*, *378*, 467–469.

[6] Mitov, M., Nouvet, E., & Dessaud, N. (2004). Polymer-stabilized cholesteric liquid crystals as switchable photonic broad bandgaps. *Eur. Phys. J. E*, *15*, 413–419.

[7] Lu, S.-Y., & Chien, L.-C. (2007). A polymer-stabilized single-layer color cholesteric liquid crystal display with anisotropic reflection. *Applied Physics Letters*, *91*, 131119.

[8] Huang, Y., Zhou, Y., Doyle, C., & Wu, S.-T. (2006). Tuning the photonic band gap in cholesteric liquid crystals by temperature-dependent dopant solubility. *Optics Express*, *14*(3), 1236–1242.

[9] Yip, W. C., & Kwok, H. S. (2001). Helix unwinding of doped cholesteric liquid crystals. *Applied Physics Letters*, *78*(4), 425–427.

[10] Belyakov, V. A. (2002). Untwisting of the helical structure in a plane layer of chiral liquid crystal. *JETP Letters*, *76*(2), 88–92.

[11] Bailey, C. A., Tondiglia, V. P., Natarajan, L. V., Duning, M. M., Bricker, R. L., Sutherland, R. L., White, T. J., Durstock, M. F., & Bunning, T. J. (2010). Electromechanical tuning of cholesteric liquid crystals. *Journal of Applied Physics*, *107*, 013105.

[12] Natarajan, L. V., Wofford, J. M., Tondiglia, V. P., Sutherland, R. L., Koerner, H., Vaia, R. A., & Bunning, T. J. (2008). Electro-thermal tuning in a negative dielectric cholesteric liquid crystal material. *Journal of Applied Physics*, *103*, 093107.

[13] Hrozhyk, U. A., Serak, S. V., Tabiryan, N. V., White, T. J., & Bunning, T. J. (2011). Nonlinear optical properties of fast, photoswitchable cholesteric liquid crystal bandgaps. *Optical Materials Express*, *1*(5), 943–952.

[14] Allahverdyan, K., & Galstian, T. (2011). Electrooptic jumps in natural helicoidal photonic bandgap structures. *Optics Express*, *19*(5), 4611–4617.

[15] Allahverdyan, K., & Galstian, T. (2011). Accelerating the cholesteric helix restoring by a dual frequency compound. Submitted to MC&LC, proceedings of OLC.

[16] Yin, Y., Gu, M., Golovin, A. B., Shiyanovskii, S. V., & Lavrentovich, O. D. (2004). Fast switching optical modulators based on dual frequency nematic cell. *Mol. Cryst. Liq. Cryst.*, *421*, 133–144.

[17] Li, W., Zhang, H., Wang, L., Ouyang, C., Ding, X., Cao, H., & Yang, H. (2007). Effect of a chiral dopant on the electro-optical properties of polymer-dispersed liquid-crystal films. *Journal of Applied Polymer Science*, DOI 10.1002/app.

[18] Merck Ltd. http://www.merck-chemicals.com/lcd-emerging-technologies.

[19] Gevoegyan, A. A., Papoyan, K. V., & Pikichyan, O. V. (2000). Reflection and transmission of light through the systems cholesteric liquid crystal-glass plate-cholesteric liquid crystal and cholesteric liquid crystal(1)-cholesteric liquid crystal(2). *Optics Spectroscopy*, *88*, 586–593.

[20] Gevorgyan, A. H. (2011). Tunable reflectance of a two-defect-layer cholesteric liquid crystal. *Phys. Rev. E.*, *83*(1), 011702(1–12).
[21] Gevorgyan, A. A. (2000). Reflection and transmission of light for a layer with dielectric and magnetic helicities. I. Jones matrices. Natural polarizations. *Optics and Spectroscopy*, *89*, 631–638.
[22] Azzam, R. M. A., & Bashara, N. M. (1977). *Ellipsometry and Polarized Light*, North-Holland: New York.